Published OnlineFirst June 22, 2010; DOI: 10.1158/0008-5472.CAN-09-4672

Microenvironment and Immunology

Cancer Research

Different Tumor Microenvironments Contain Functionally Distinct Subsets of Macrophages Derived from Ly6C(high) Monocytes

Kiavash Movahedi[1,2], Damya Laoui[1,2], Conny Gysemans[4], Martijn Baeten[1,2], Geert Stangé[3], Jan Van den Bossche[1,2], Matthias Mack[5], Daniel Pipeleers[3], Peter In't Veld[3], Patrick De Baetselier[1,2], and Jo A. Van Ginderachter[1,2]

Abstract

Tumor-associated macrophages (TAM) form a major component of the tumor stroma. However, important concepts such as TAM heterogeneity and the nature of the monocytic TAM precursors remain speculative. Here, we show for the first time that mouse mammary tumors contained functionally distinct subsets of TAMs and provide markers for their identification. Furthermore, in search of the TAM progenitors, we show that the tumor-monocyte pool almost exclusively consisted of $Ly6C^{hi}CX_3CR1^{low}$ monocytes, which continuously seeded tumors and renewed all nonproliferating TAM subsets. Interestingly, gene and protein profiling indicated that distinct TAM populations differed at the molecular level and could be classified based on the classic (M1) versus alternative (M2) macrophage activation paradigm. Importantly, the more M2-like TAMs were enriched in hypoxic tumor areas, had a superior proangiogenic activity *in vivo*, and increased in numbers as tumors progressed. Finally, it was shown that the TAM subsets were poor antigen presenters, but could suppress T-cell activation, albeit by using different suppressive mechanisms. Together, our data help to unravel the complexities of the tumor-infiltrating myeloid cell compartment and provide a rationale for targeting specialized TAM subsets, thereby optimally "re-educating" the TAM compartment. *Cancer Res; 70(14); 5728–39. ©2010 AACR.*

Introduction

Myeloid cells are frequently found to infiltrate tumors and have been linked to diverse tumor-promoting activities (1). In particular, tumor-associated macrophages (TAM) are an important component of the tumor stroma, both in murine models and human patients (2). TAMs can promote tumor growth by affecting angiogenesis, immune suppression, and invasion and metastasis (2, 3). However, it seems unlikely that these diverse functions are performed by a single cell type, and the existence of distinct TAM subsets, linked to different intratumoral microenvironments, has been predicted (4). Nevertheless, studies identifying spatially and functionally distinct TAM subpopulations are currently lacking.

Authors' Affiliations: [1]Cellular and Molecular Immunology, Department of Molecular and Cellular Interactions, VIB; [2]Cellular and Molecular Immunology and [3]Diabetes Research Center, Vrije Universiteit Brussel, Brussels, Belgium; [4]Experimental Medicine and Endocrinology, Department of Experimental Medicine, Katholieke Universiteit Leuven, Leuven, Belgium; and [5]Department of Internal Medicine, University of Regensburg, Regensburg, Germany

Note: Supplementary data for this article are available at Cancer Research Online (http://cancerres.aacrjournals.org/).

Corresponding Author: Jo A. Van Ginderachter, Vrije Universiteit Brussel, CMIM, Building E8, Pleinlaan 2, B-1050 Brussels, Belgium. Phone: 32-2-6291978; Fax: 32-2-6291981; E-mail: jvangind@vub.ac.be.

doi: 10.1158/0008-5472.CAN-09-4672

Tissue-resident macrophages can be maintained through local proliferation or differentiation *in situ* from circulating monocytic precursors (5). Importantly, discrete subsets of blood monocytes have been described. Mouse monocytes can be classified as $Ly6C^{low}CX_3CR1^{hi}$ ($CCR2^-CD62L^-$) or $Ly6C^{hi}CX_3CR1^{low}$ ($CCR2^+CD62L^+$) and are shown to have distinct functions and migration patterns (6). However, information on the nature and dynamics of the monocytic TAM precursors is lacking thus far.

Macrophages are plastic cells that can adopt different phenotypes depending on the immune context. Microenvironmental stimuli can drive a macrophage either toward a "classic" (M1) or an "alternative" (M2) activation state, two extremes in a spectrum (7). M1 macrophages are typically characterized by the expression of proinflammatory cytokines, inducible nitric oxide synthase 2 (*Nos2*), and MHC class II molecules. M2 macrophages have a decreased level of the aforementioned molecules and are identified by their signature expression of a variety of markers, including arginase-1 and mannose and scavenger receptors. It has been suggested that TAMs display an M2-like phenotype (8), although it is not clear whether these findings can be generalized and are applicable to TAMs in different tumor regions. In addition, the processes and signaling pathways that are driving the M2 phenotype of TAMs are not yet fully understood. A factor that is believed to be crucial in shaping the TAM phenotype is tumor hypoxia (9). Although hypoxia is known to have dramatic effects on the activation

Published OnlineFirst June 22, 2010; DOI: 10.1158/0008-5472.CAN-09-4672

and function of macrophages, it remains to be determined how this relates to the M2-like orientation of TAMs.

In this study, we show the existence of molecularly and functionally distinct TAM subsets, located in different intratumoral regions, and uncover Ly6C^{hi} monocytes as their precursors. These results might prove important for therapeutic interventions targeted at specific TAM subsets or their precursors.

Materials and Methods

Mice, cell lines

Female BALB/c and C57BL/6 mice were from Harlan. BALB/c CX$_3$CR1$^{GFP/GFP}$ mice were provided by Dr. Grégoire Lauvau (Université de Nice-Sophia Antipolis, Nice, France). The BALB/c mammary adenocarcinoma TS/A (10) was provided by Dr. Vincenzo Bronte (Istituto Oncologico Veneto, Padova, Italy); BALB/c 4T1 mammary carcinoma (11) was provided by Dr. Massimiliano Mazzone (VIB-KULeuven, Leuven, Belgium); and 3LL-R clone of the C57BL/6 Lewis Lung carcinoma was derived as described previously (12). Cells were injected subcutaneously (s.c.) in the flank (3×10^6) or in the mammary fat pad (10^6).

Tumor preparation, fluorescence-activated cell sorting

Tumors were treated with 10 U/mL collagenase I, 400 U/mL collagenase IV, and 30 U/mL DNaseI (Worthington). Density gradients (Axis-Shield) were used to remove debris and dead cells. To purify TAMs, CD11b$^+$ cells were MACS-enriched (anti–CD11b microbeads, Miltenyi Biotec) and sorted using a BD FACSAria II (BD Biosciences). To purify dendritic cells, spleens were flushed with 200 U/mL collagenase III (Worthington). CD11c$^+$ cells were MACS-enriched (anti-CD11c microbeads, Miltenyi Biotec), and CD11c$^+$MHC II^{hi}B220$^-$Ly6C$^-$ dendritic cells were sorted.

Antibodies used are listed in Supplementary Table S1.

For tumor necrosis factor α (TNFα) stainings, TAMs were cultured 5 hours with Brefeldin A (BD Biosciences). For inducible nitric oxide synthase (iNOS), TAMs were cultured with 10 U/mL IFNγ and/or 10 ng/mL lipopolysaccharide (LPS) for 12 hours.

Arginase activity was measured as described earlier (13).

In vivo monocyte labeling

Latex labeling of monocytes was described earlier (14, 15). For Ly6C^{low} monocyte labeling, mice were injected intravenously (i.v.) with 250 μL 0.5 μm yellow-green microspheres (Polysciences; 1:25). Twenty-four hours later, TS/A was injected s.c. For Ly6C^{hi} monocyte labeling, mice were injected i.v. with 250 μL clodronate liposomes (16) and 18 hours later with latex microspheres (i.v.) and TS/A (s.c.).

Bromodeoxyuridine staining, cell cycle analysis

Mice were injected intraperitoneally with 1 mg bromodeoxyuridine (BrdUrd) (Sigma), and 0.8 mg/mL BrdUrd was administered to drinking water. To stain for BrdUrd, Ki67 (BD Biosciences), or propidium iodide (Invitrogen), cells were fixed/permeabilized using the BD Biosciences BrdUrd labeling kit.

RNA extraction, cDNA preparation, and quantitative reverse transcriptase-PCR

These tests were performed as described earlier (17). Gene-specific primers are listed in Supplementary Table S2.

Immunohistochemistry, hypoxia measurements

For hypoxia stainings, mice were injected with 80 mg/kg body weight pimonidazole [hypoxyprobe-1 (HP-1), HPI, Inc.]. Two hours later, tumors were snap frozen, sections were acetone fixed, and stained. Pictures were acquired with a Plan-Neofluar 10×/0.30 or Plan-Neofluar 20×/0.50 (Carl Zeiss) objective on a Zeiss Axioplan 2 microscope equipped with an Orca-R2 camera (Hamamatsu) and Smartcapture 3 software (Digital Scientific UK). For HP-1 fluorescence-activated cell sorting (FACS) measurements, cells were fixed/permeabilized using the BD Biosciences Fix/Perm kit and rat anti–HP-1/FITC (HPI) was added (30–37°C).

Chorioallantoic membrane assays

Chorioallantoic membrane (CAM) assays were performed as described earlier (18). Gelatin sponges (1–2 mm^3; Hospithera) with 5×10^4 sorted TAM subsets were placed on the CAM. PBS/0.1% bovine serum albumin (BSA; 50 μg/CAM) and recombinant human vascular endothelial growth factor (VEGF)-A$_{165}$ (5 μg/CAM) served as controls. At day 13, membranes were fixed and analyzed using a Zeiss Lumar V.12 stereomicroscope with NeoLumar S 1.5× objective (15× magnification).

Mixed leukocyte reaction, suppression assays

For allo–mixed leukocyte reaction (MLR) assays, 2×10^5 MACS-purified CD4$^+$/CD8$^+$ C57BL/6 T cells were added to 5×10^4 sorted TAMs or conventional dendritic cells and 3 days later were [^{3}H]thymidine pulsed.

For T-cell suppression assays, 1×10^5 to 1.25×10^4 (1:2–1:16) sorted TAMs/conventional dendritic cells were added to 2×10^5 naive BALB/c splenocytes with 1 μg/mL anti-CD3 and were [^{3}H]thymidine pulsed 24 hours later. L-NMMA (0.5 mmol/L, Sigma) and/or NorNoha (0.5 mmol/L, Calbiochem) were added in a 1:4 ratio. Relative percent suppression of proliferation was calculated as described earlier (19).

Statistics

Significance was determined by Student's *t* test.

Results

TS/A tumors are highly infiltrated with a heterogeneous population of myeloid cells containing distinct granulocyte and monocyte/macrophage subsets

To study the tumor-infiltrating myeloid compartment, we, at first instance, used the BALB/c mammary adenocarcinoma model TS/A. Subcutaneous tumors contained a large CD11b$^+$ fraction, indicating a high infiltration of myeloid cells (Fig. 1A). Interestingly, this CD11b$^+$ population was heterogeneous and encompassed at least seven subsets, which could be readily distinguished based on their differential expression of MHC class II and Ly6C (Fig. 1A). Ly6C^{hi}MHC II$^-$ cells (gate 1: Fig. 1A) were F4/80$^+$CX$_3$CR1^{low}CCR2^{hi}CD62L$^+$, did not express

Published OnlineFirst June 22, 2010; DOI: 10.1158/0008-5472.CAN-09-4672

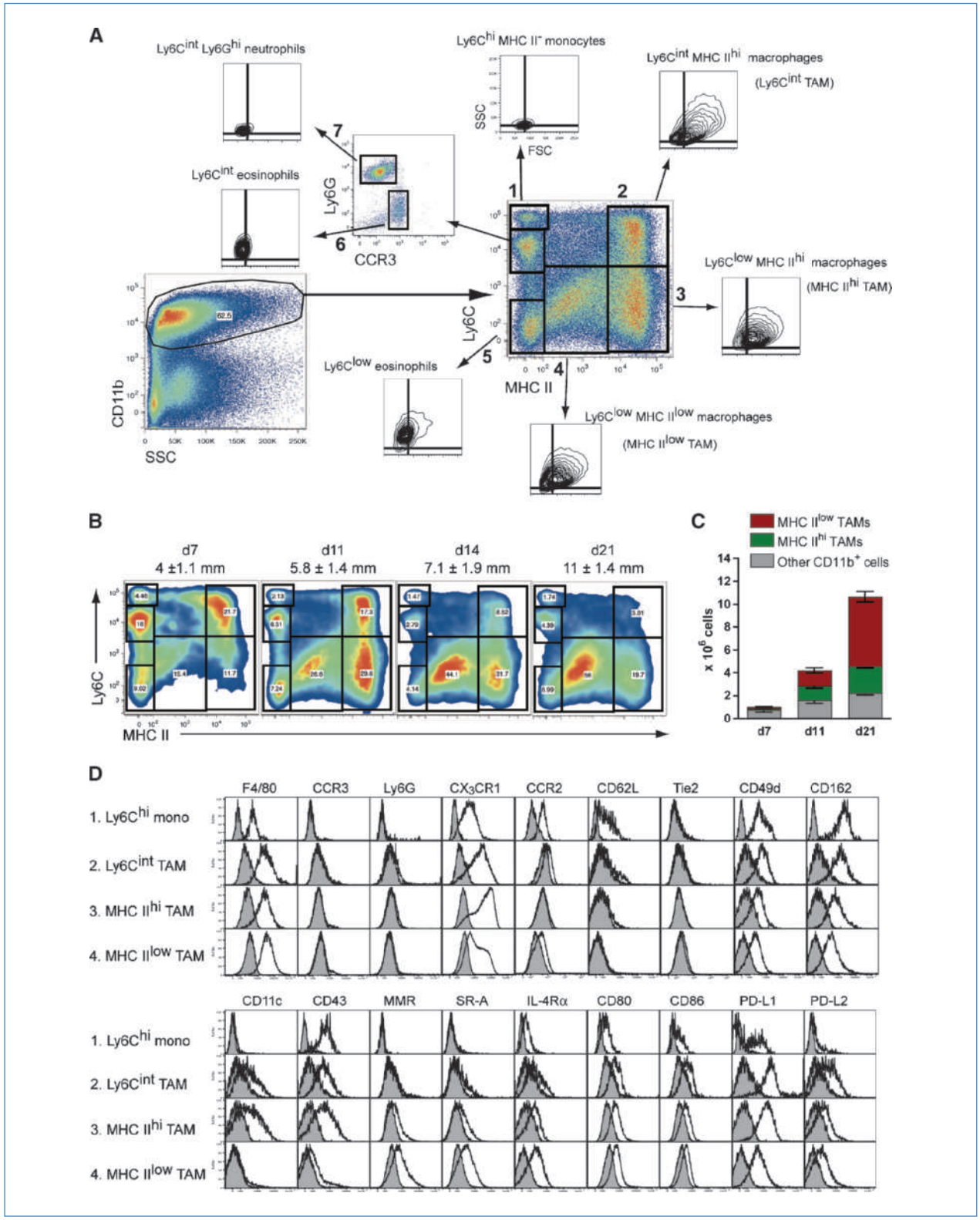

Figure 1. TS/A tumors are infiltrated by distinct granulocyte and monocyte/macrophage subsets. A, identification of distinct myeloid subsets in single-cell suspensions of 11-d-old tumors (n = 4). B, subsets in gated CD11b$^+$ cells from 7-, 11-,14-, and 21-d-old tumors. Tumor diameters are shown (n = 3). C, numbers of TAM subsets at different time points. D, expression of indicated markers on TAM subsets. For CX_3CR1, tumors were grown in $CX_3CR1^{GFP/+}$ mice. Shaded histograms, isotype control (n = 6).

Published OnlineFirst June 22, 2010; DOI: 10.1158/0008-5472.CAN-09-4672

the granulocyte markers Ly6G or CCR3, and had a small size and granularity ($FSC^{low}SSC^{low}$), indicating that they were Ly6-C^{hi} monocytes (Fig. 1A and D; Supplementary Fig. S1). The $CD11b^{+}$MHC II^{+} cells in gates 2 to 4 were reminiscent of macrophages, having an enlarged macrophage-like scatter and expressing high levels of F4/80 (Fig. 1A and D). Remarkably, distinct subsets of TAMs were clearly distinguishable: $Ly6C^{int}$MHC II^{hi} ($Ly6C^{int}$ TAMs, gate 2), $Ly6C^{low}$MHC II^{hi} (MHC II^{hi} TAMs, gate 3), and $Ly6C^{low}$MHC II^{low} (MHC II^{low} TAMs, gate 4). The majority of $Ly6C^{low}$MHC II^{-} cells were $CCR3^{+}CX_3CR1^{-}$ eosinophils (Fig. 1A, gate 5; Supplementary Fig. S1, gate E). However, $Ly6C^{low}$MHC II^{-} cells also consisted of $CCR3^{-}CX_3CR1^{low}$ (Supplementary Fig. S1, gate 2) and $CCR3^{-}CX_3CR1^{hi}$ (Supplementary Fig. S1, gate 3) cells, the latter possibly resembling $Ly6C^{low}CX_3CR1^{hi}$ monocytes. However, the majority of these CX_3CR1^{hi} cells did not have a monocyte scatter, suggesting they were TAMs (Supplementary Fig. S1). This suggests that $Ly6C^{low}$ monocytes were not present in significant amounts in these tumors. Finally, TS/A tumors were also infiltrated with $CCR3^{+}Ly6C^{int}$ eosinophils (Fig. 1A, gate 6) and $Ly6G^{hi}$ neutrophils (Fig. 1A, gate 7).

Interestingly, the relative percentages of these distinct myeloid subpopulations dramatically changed as tumors progressed (Fig. 1B). Within the TAM compartment, the percentage of $Ly6C^{int}$ TAMs decreased, whereas the Ly6-C^{low}MHC II^{low} TAM subset became gradually more prominent, reaching up to 60% of the myeloid tumor infiltrate in large tumors (>10 mm). Because the amount of tumor-infiltrating $CD11b^{+}$ cells increased as tumors progressed (Fig. 1C), MHC II^{low} TAMs also strongly accumulated in absolute numbers, to a much greater extent than MHC II^{hi} TAMs.

$Ly6C^{hi}$ monocytes are the precursors of all TAM subsets in TS/A tumors

Macrophages typically derive from circulating blood-borne precursors such as monocytes. The presence of $Ly6C^{hi}$, but not $Ly6C^{low}$, monocytes in TS/A tumors suggested that the former could be more efficiently recruited to tumors and function as the TAM precursor. To investigate this, we selectively labeled $Ly6C^{hi}$ or $Ly6C^{low}$ monocyte subsets *in vivo* with fluorescent latex beads, using a previously described procedure (14, 15). This method has been validated to stably label the respective monocyte subsets for 5 to 6 days in naive mice. Hence, TS/A was injected after $Ly6C^{low}$ or $Ly6C^{hi}$ monocyte labeling, and tumors were collected 6 days post injection. No appreciable numbers of tumor-infiltrating $latex^{+}$ monocytes were observed when applying the $Ly6C^{low}$-labeling strategy (Fig. 2A). In contrast, $Ly6C^{hi}$ labeling resulted in the detection of a significant fraction of $CD11b^{+}latex^{+}$ monocytes, illustrating that $Ly6C^{hi}$ monocytes comprise the main tumor-infiltrating monocyte subset. With this approach, $latex^{+}$ cells could be detected up to 19 days after tumor injection (Fig. 2B), allowing a follow-up of the monocyte progeny in the course of tumor growth. At day 6, $latex^{+}Ly6C^{hi}$ monocytes had differentiated into $latex^{+}Ly6C^{int}$ TAMs, and to some extent also into $latex^{+}$MHC II^{hi} and $latex^{+}$MHC II^{low} TAMs (Fig. 2B). From day 12 onward, the majority of $latex^{+}$ $Ly6C^{hi}$ monocytes had converted into $latex^{+}$MHC II^{hi} and $latex^{+}$MHC II^{low} TAMs. Together, these data show that all TAM subsets can be derived from $Ly6C^{hi}$ monocytes.

Remarkably, the total number of peripheral blood monocytes had significantly increased at later stages of tumor growth (≥21 days post injection; Supplementary Fig. S2A). Furthermore, around 4 weeks of tumor growth, there was a significant increase in the percentage of the $Ly6C^{hi}$ monocyte subset (Supplementary Fig. S2B–C).

$Ly6C^{int}$, MHC II^{hi}, and MHC II^{low} TAMs have distinct differentiation kinetics and turnover rates

To determine the turnover rate and differentiation kinetics of the monocyte/TAM subsets, BrdUrd was administered continuously to tumor-bearing animals and its incorporation was measured at consecutive time points. Tumor-infiltrating $Ly6C^{hi}$ monocytes quickly became $BrdUrd^{+}$, reaching plateau values after 48 hours of BrdUrd administration (Fig. 2C). This indicates a rapid monocyte turnover rate and/or proliferation of monocytes inside tumors. Remarkably, although intratumoral $Ly6C^{hi}$ monocytes were $Ki67^{+}$ (Fig. 2D1), none were found to be in the S-G_2-M phase (Fig. 2D2), suggesting that these cells were in the G_1 phase and not proliferating (20). TAMs were $Ki67^{-}$, and no appreciable numbers were found in S-G_2-M phase, indicating no significant levels of proliferation. Hence, TAMs were unable to directly incorporate BrdUrd so that $BrdUrd^{+}$ TAMs must differentiate from $BrdUrd^{+}$ monocytes, resulting in a lag phase of BrdUrd positivity. Indeed, only a minor fraction of MHC II^{hi} and MHC II^{low} TAMs were $BrdUrd^{+}$ upon 24 hours of BrdUrd administration (Fig. 2C). However, compared with these subsets, Ly6-C^{int} TAMs incorporated BrdUrd at a faster rate, with a higher percentage being $BrdUrd^{+}$ already at 24 hours. These results suggest that monocytes first give rise to $Ly6C^{int}$ TAMs, which then differentiate into MHC II^{hi} and MHC II^{low} TAMs. MHC II^{hi} and MHC II^{low} TAMs incorporated BrdUrd slowly and with similar kinetics, arguing for a comparable and low turnover rate.

MHC II^{hi} and MHC II^{low} TAMs differ at the molecular level

Although efforts have previously been made to characterize TAMs at the molecular level (21, 22), a thorough study of TAM heterogeneity is lacking up to now. Hence, we further characterized the distinct TAM subsets at the gene and protein levels. Gene expression of sorted MHC II^{hi} and MHC II^{low} TAMs (Supplementary Fig. S3A) was analyzed through quantitative reverse transcriptase-PCR (RT-PCR; Table 1). $Ly6C^{int}$ TAMs, constituting only a minor fraction in larger tumors, were not included in this analysis. Interestingly, when comparing MHC II^{hi} with MHC II^{low} TAMs (Table 1, hi/low), M2-associated genes such as *Arg1* (arginase-1), *Cd163, Stab1* (stabilin-1), and *Mrc1* (MMR) were higher expressed in the MHC II^{low} subset. In contrast, more M1-type, proinflammatory genes, such as *Nos2 (iNOS), Ptgs2 (Cox2), Il1b, Il6*, and *Il12b*, were upregulated in MHC II^{hi} TAMs. This differential activation state was also reflected at the protein level. Membrane expression of the M2 markers macrophage mannose receptor (MMR), macrophage scavenger receptor 1 (SR-A),

Published OnlineFirst June 22, 2010; DOI: 10.1158/0008-5472.CAN-09-4672

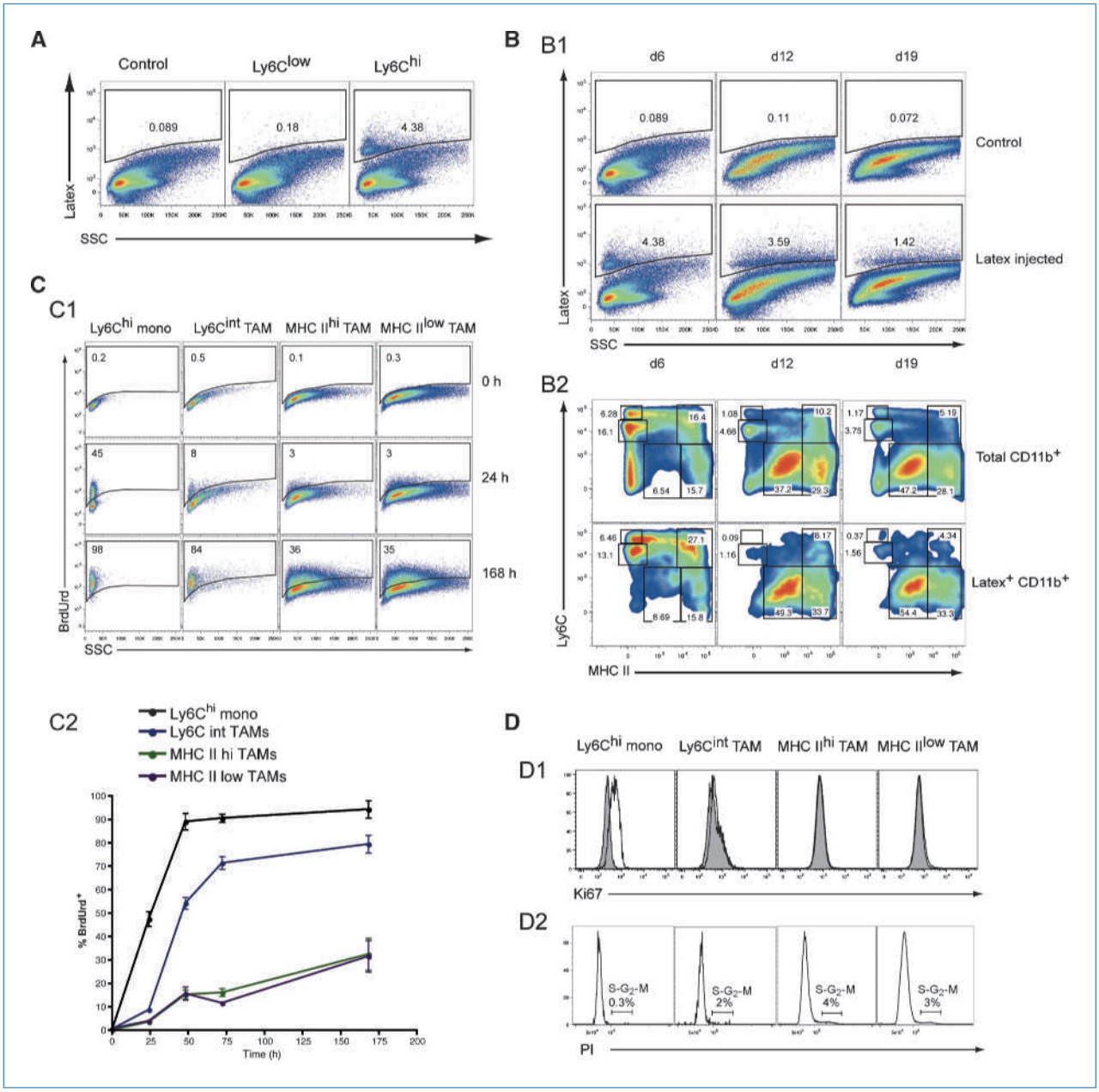

Figure 2. Infiltration of latex-labeled monocytes in tumors and kinetics of BrdUrd incorporation in TAM subsets. A, 6-d-old tumors were collected from control mice or Ly6C^{low} or Ly6C^{hi} monocyte-labeled mice. Plots are gated on CD11b$^+$ cells (n = 3). B, 6-, 12-, or 19-d-old tumors were collected from untreated mice (control) or Ly6C^{hi} monocyte–labeled mice (latex injected). Plots are gated on CD11b$^+$ cells (n = 3). C, 2-wk tumor-bearing mice were left untreated (0 h) or given BrdUrd for the indicated time (n = 2). D, D1, intracellular expression of Ki67. Shaded histograms, isotype controls. D2, DNA staining with propidium iodide. Gate represents percentage of cells in S-G_2-M phase (n = 3).

and interleukin-4Rα (IL-4Rα) were clearly higher on MHC II^{low} TAMs, whereas the M1-associated marker CD11c was only expressed on MHC II^{hi} TAMs (Fig. 1D). Moreover, although arginase activity was observed in both TAM subsets, it was significantly higher for MHC II^{low} TAMs (Fig. 3A). In the same vein, TNFα, which has previously been reported to associate with a M2 phenotype in tumors (23, 24), was produced by both TAM subsets; however, a significantly higher percentage of MHC II^{low} TAMs were found to be TNFα$^+$ (Fig. 3B). Although iNOS protein was not detected in freshly isolated TAMs, it could be induced by IFN-γ and/or LPS stimulation (Fig. 3C). Interestingly, IFN-γ or LPS induced iNOS more efficiently in MHC II^{hi} TAMs, with a higher fraction of these cells becoming iNOS$^+$. Together, these data indicate that the identified TAM subsets have a differential activation state, with MHC II^{low} TAMs being more M2 oriented.

Published OnlineFirst June 22, 2010; DOI: 10.1158/0008-5472.CAN-09-4672

Table 1. Gene expression profile of MHC II^{hi} versus MHC II^{low} TAMs from TS/A tumors

Gene	Hi/low	Hi/low (90% CI)	*P*	ΔC_T hi
Ccl17		30 (19–47)	**	8.1 ± 0.3
Cx3cl1		9.2 (4.4–19)	*	12.2 ± 0.5
Cxcl11		7.4 (4.2–13)	**	9.2 ± 0.1
Ccl5		6.1 (4.1–8.9)	*	5.4 ± 0.4
Il6		5.9 (1.8–19)		14 ± 0.9
Cxcl10		5.9 (4.3–8.2)	*	5.4 ± 0.4
Cxcl9		5.3 (4.2–6.6)	***	6.4 ± 0.0
Il12b		4.0 (1.6–10)		12.4 ± 0.4
Il1b		3.6 (2.6–5.1)	***	2.9 ± 0.1
Pgf		3.3 (0.68–16)		9.5 ± 0.5
Mmp9		2.9 (1.9–4.2)		4.0 ± 0.5
Ptgs2 (Cox2)		2.3 (1.1–5.0)		7.3 ± 0.6
Nos2 (iNOS)		2.3 (1.4–3.8)	*	8.8 ± 0.1
Angpt2		2.1 (1.6–2.7)	**	9.2 ± 0.1
Ccl22		2.0 (1.9–2.2)	*	11.5 ± 0.3
Tek (Tie2)		1.8 (1.5–2.2)		5.7 ± 0.4
Vegfa		1.6 (1.3–2.0)		6.2 ± 0.2
Thbs2 (TSP2)		1.2 (0.9–1.8)		13 ± 0.0
Il1a		1.2 (1.0–1.3)		6.8 ± 0.4
Il10		1.0 (0.69–1.5)		9.2 ± 0.3
Cxcl16		0.97 (0.67–1.4)		4.1 ± 0.0
Tnf		0.93 (0.64–1.3)		5.1 ± 0.3
Thbs1 (TSP1)		0.89 (0.79–1.00)		6.2 ± 0.2
Cx3cr1		0.85 (0.63–1.2)		7.4 ± 0.2
Mif		0.79 (0.67–0.93)		3.9 ± 0.1
Igf1		0.78 (0.63–0.97)		10.3 ± 0.4
Mmp14		0.77 (0.53–1.1)		8.3 ± 0.1
Ccr2		0.71 (0.39–1.3)		6.5 ± 0.5
Plau (uPA)		0.71 (0.62–0.81)		5.7 ± 0.1
Ccl11		0.7 (0.39–1.2)		12.6 ± 0.3
Adamts1		0.68 (0.44–1.0)		14.1 ± 0.3
Ccl1		0.65 (0.43–0.99)		12.5 ± 0.5
Tgfb1		0.64 (0.58–0.70)	*	4.5 ± 0.2
Cxcl1		0.64 (0.51–0.79)		3.5 ± 0.4
Ccl8		0.57 (0.33–0.98)		6.5 ± 0.4
Il4ra		0.50 (0.44–0.57)		10.6 ± 0.2
Arg1		0.48 (0.46–0.51)	**	1.7 ± 0.1
Spp1		0.45 (0.40–0.51)	*	1.0 ± 0.1
Ccl12		0.44 (0.30–0.64)	*	2.7 ± 0.2
Ccl6		0.39 (0.27–0.57)	*	1.9 ± 0.3
Ccl4		0.34 (0.24–0.48)	**	4.8 ± 0.4
Ctsd		0.33 (0.30–0.36)	**	4.4 ± 0.2
Ccl9		0.33 (0.27–0.39)	**	2.5 ± 0.3
Ccl3		0.33 (0.25–0.43)	**	6.0 ± 0.2
Timp2		0.30 (0.15–0.59)	*	4.8 ± 0.5
Ccl2		0.26 (0.19–0.36)	*	2.7 ± 0.4
Ccl7		0.25 (0.18–0.35)	**	2.9 ± 0.5
Mrc1 (MMR)		0.23 (0.21–0.25)	***	4.2 ± 0.0
Stab1		0.22 (0.16–0.29)	**	5.5 ± 0.2
CD163		0.16 (0.12–0.21)	**	9.6 ± 0.1
Lyve1		0.033 (0.019–0.06)	*	8.5 ± 0.1

NOTE: Gene expression was assessed using quantitative RT-PCR and normalized based on S12 and is shown as the relative expression in MHC II^{hi} versus MHC II^{low} TAMs (hi/low). Values are geometric means of three to four independent experiments. Accompanying 90% confidence intervals (90% CI) and *P* values are shown: *, $P < 0.05$; **, $P < 0.01$; ***, $P < 0.001$. C_T = threshold cycle. ΔC_T (calculated for MHC II^{hi} TAMs) = C_T(gene) – C_T(S12); lower ΔCt, corresponds to higher expression levels. , >5; , 2–5; , 0.5–2; , 0.5–0.2; , <0.2.

TAM subsets also showed a markedly distinct chemokine expression pattern (Table 1). Notably, mRNAs for chemokines typically involved in lymphocyte attraction, such as *Ccl5, Cx$_3$cl1, Cxcl11, Cxcl10, Cxcl9*, and the CCR4 ligands *Ccl17* and *Ccl22* were upregulated in MHC II^{hi} TAMs. In contrast, mRNAs for monocyte/macrophage chemoattractants, such as *Ccl6*; the CCR2 ligands *Ccl7, Ccl2*, and *Ccl12*; and the CCR5/CCR1 ligands *Ccl4, Ccl3*, and *Ccl9* were significantly higher in MHC II^{low} TAMs. Furthermore, at the protein level, a differential expression of the chemokine receptors CX$_3$CR1 and CCR2 was observed, with MHC II^{hi} TAMs being CX$_3$CR1^{hi}CCR2$^-$, whereas MHC II^{low} TAMs were CX$_3$CR1^{low}CCR2$^+$ (Fig. 1D).

Both TAM subsets expressed many potentially proangiogenic genes, including *Vegfa, Mmp9, Pgf, Spp1*, and *cathD* (Table 1). However, several angiostatic factors such as *angpt2, Cxcl9, Cxcl10*, and *Cxcl11* were upregulated in the MHC II^{hi} fraction. One of the most differentially expressed genes (higher in MHC II^{low} TAMs) was *Lyve1*, a marker previously associated with angiogenic/hypoxic macrophages (25).

We conclude that MHC II^{hi} and MHC II^{low} TAMs have a distinguishing profile of molecules involved in inflammation (M1/M2), chemotaxis, and angiogenesis.

Differentially activated MHC II^{hi} and MHC II^{low} TAMs infiltrate 4T1 mammary and 3LL lung carcinomas

To extrapolate these findings to orthotopically grown tumors, TS/A was injected in the mammary fat pad. Orthotopic

Published OnlineFirst June 22, 2010; DOI: 10.1158/0008-5472.CAN-09-4672

tumors contained identical myeloid subsets, which accumulated with comparable kinetics (Supplementary Fig. S4A) and retained their differential expression of surface markers (Supplementary Fig. S4B).

We then investigated whether differentially activated TAM subsets were present in other tumor models. Interestingly, orthotopic 4T1 mammary and subcutaneous 3LL lung carcinoma tumors contained distinct granulocyte and monocyte/macrophage subsets (Supplementary Figs. S5A and S6A), including Ly6C^{hi} monocytes (gate 1), Ly6C^{int} TAMs (gate 2), MHC II^{hi} TAMs (gate 3), and MHC II^{low} TAMs (gate 4). 3LL tumors also contained a population of Ly6C^{int}MHC II^{low} TAMs (Supplementary Fig. S6A, gate 5), possibly representing an alternative differentiation path from Ly6C^{hi} monocytes to Ly6C^{low} TAMs. As with TS/A, the progression of 3LL tumors was linked with an accumulation of MHC II^{low} TAMs (Supplementary Fig. S6B). Surprisingly, progressing 4T1 tumors gradually increased their MHC II^{hi} TAM content (Supplementary Fig. S5B), indicating that the relative increase of TAM subsets over time is tumor dependent.

Interestingly, the 4T1 and 3LL tumor-derived MHC II^{hi} and MHC II^{low} TAM subsets remained differentially M1- versus M2-like activated, shown by enhanced M2 marker gene expression in MHC II^{low} TAMs (*CD163, Stab1, Arg1, Mrc1, IL4Ra, Il10*) and M1 marker upregulation in MHC II^{hi} TAMs (*Il1b, Il12b, Cox2*; Supplementary Tables S3 and S4). Of note, although *Nos2* mRNA was higher in the 3LL MHC II^{low} TAMs, iNOS protein levels were higher in MHC II^{hi} TAMs, supporting their more M1-like activation (Supplementary Fig. S7). Finally, in both models, MHC II^{low} TAMs expressed higher levels of MMR and IL4Rα protein, whereas CD11c was restricted to MHC II^{hi} TAMs (Supplementary Figs. S5C and S6C). Hence, TAM subsets in three unrelated tumor models had a high level of similarity, with a consistent differential activation of MHC II^{hi} and MHC II^{low} TAMs.

MHC II^{low} TAMs are enriched in regions of hypoxia, whereas MHC II^{hi} TAMs are mainly normoxic

Tumors often harbor regions of hypoxia, a factor that is known to influence macrophage function (9). To visualize hypoxia in TS/A tumors, tumor-bearing mice were injected with pimonidazole (HP-1) and tumor sections were stained for hypoxic adducts and blood vessels. Figure 4A shows that tumors indeed contained a large number of hypoxic cells, primarily in regions with a less developed vasculature. Interestingly, staining sections for HP-1, CD11b, and MHC II showed that many CD11b$^+$MHC II$^-$ cells (which in large tumors are mainly MHC II^{low} TAMs) were HP-1$^+$ (Fig. 4B). Interestingly however, the majority of CD11b$^+$MHC II$^+$ cells were HP-1$^-$. This indicates that whereas a significant fraction of MHC II^{low} TAMs resided in hypoxic areas, MHC II^{hi} TAMs were mainly normoxic. Importantly, HP-1 adducts could also be detected through intracellular flow cytometry on freshly isolated TAMs. Again, the highest signal was seen in MHC II^{low} TAMs, confirming they were the most hypoxic TAM subset (Fig. 4C).

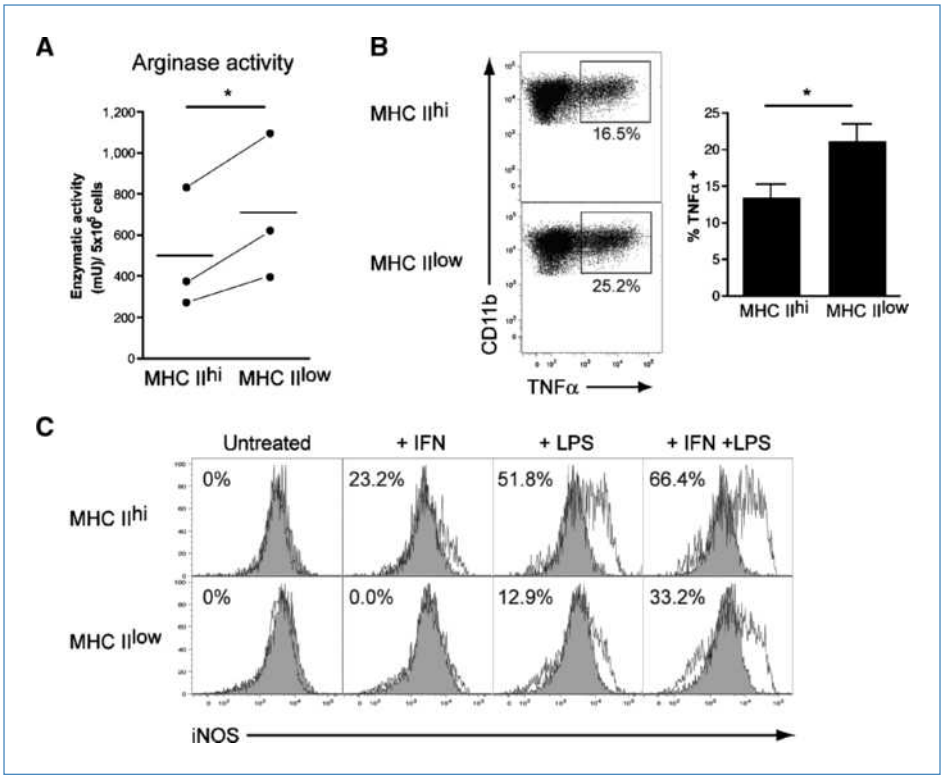

Figure 3. Arginase, TNFα, and iNOS protein expression in TAM subsets. A, arginase enzymatic activity (mU) in lysates of TAM subsets (n = 3). B, intracellular TNFα staining on TAMs. Values are means ± SEM from n = 3. C, intracellular iNOS staining on TAMs after 12-h IFNγ, LPS, or LPS + IFNγ treatment. Values represent normalized ΔMFI [= MFI (iNOS) – MFI(isotype)/MFI(iNOS) × 100], n = 2.

Published OnlineFirst June 22, 2010; DOI: 10.1158/0008-5472.CAN-09-4672

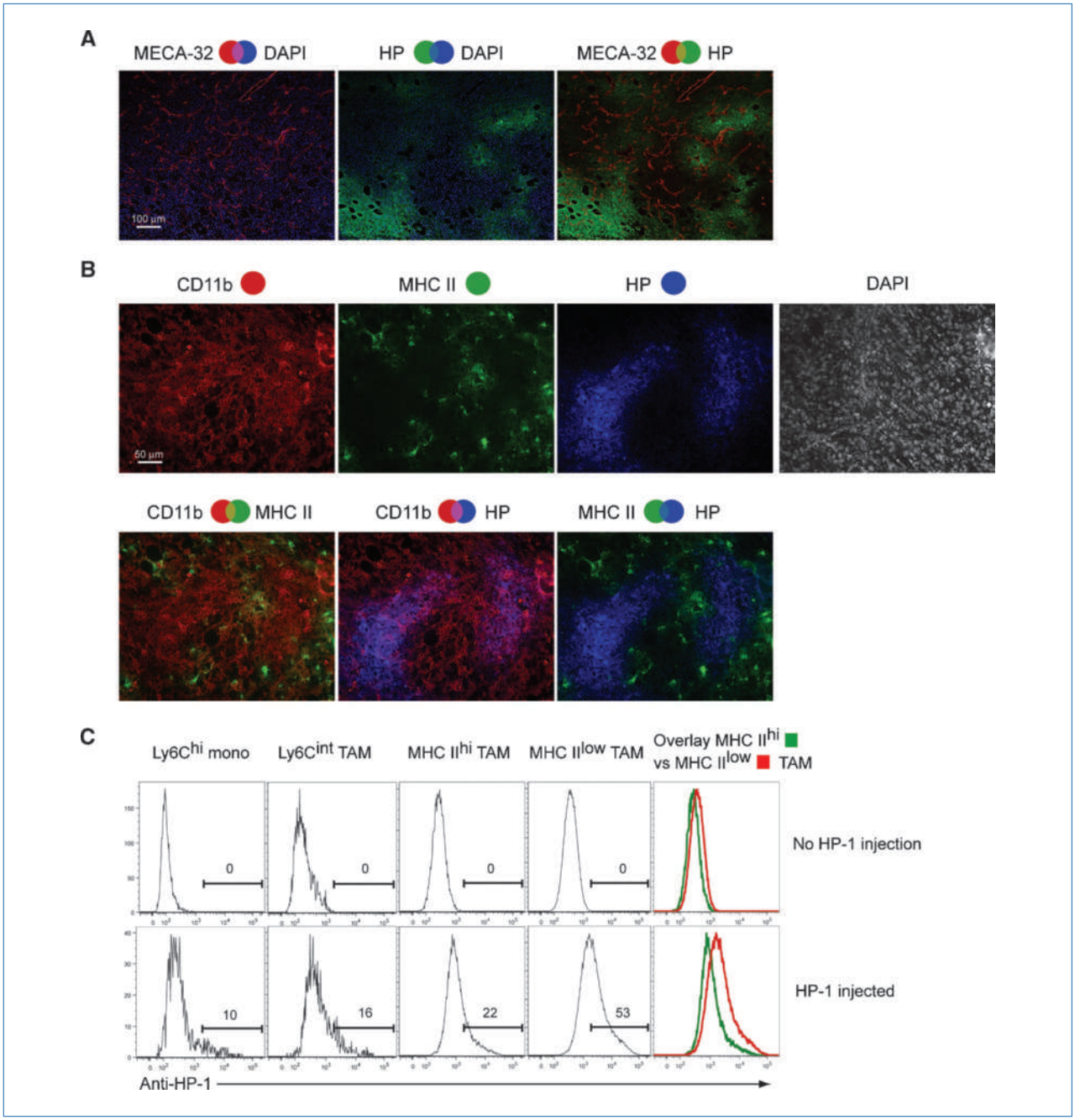

Figure 4. MHC II^{low} TAMs are enriched in hypoxic regions; MHC II^{hi} TAMs are mainly normoxic. A, 3-wk tumor-bearing mice were injected with HP-1. Tumor sections were stained with MECA32, anti–HP-1, and 4′,6-diamidino-2-phenylindole (DAPI; n = 3). B, sections were stained for CD11b, MHC II, HP-1, and DAPI (n = 3). C, HP-1 adducts in TAM subsets using intracellular FACS (n = 4).

A consequence of MHC II^{low} TAMs being in hypoxic regions should be a reduced access to blood-transported molecules. To test this, fluorescent latex particles were injected i.v. in tumor-bearing mice. One to 2 hours later, a fraction of tumor-associated CD11b^{+} cells were found to be latex^{+} (Supplementary Fig. S8A). However, latex uptake was not equal in all TAM subsets. Indeed, in relative terms, MHC II^{low} TAMs phagocytosed less latex than monocytes and other TAM subsets. This was not due to an inherently reduced phagocytic capacity of MHC II^{low} TAMs because the latter showed the highest phagocytic latex uptake *in vitro* (Supplementary Fig. S8B). These data suggest that the reduced *in vivo* latex uptake of MHC II^{low} TAMs was due to a restricted access to latex particles, which further substantiates the enrichment of MHC II^{low} TAMs in hypoxic regions.

Published OnlineFirst June 22, 2010; DOI: 10.1158/0008-5472.CAN-09-4672

MHC II^{low} TAMs show a superior proangiogenic activity *in vivo*

Hypoxia initiates an angiogenic program (26). In addition, our gene profiling revealed the expression of angiogenesis-regulating molecules in TAMs. To directly test the proangiogenic activity of both TAM subsets *in vivo*, we used the CAM assay. Sorted MHC II^{hi} or MHC II^{low} TAMs were implanted on developing CAMs, whereas BSA or rhVEGF served as negative and positive controls, respectively. rhVEGF induced the outgrowth of allantoic vessels specifically directed toward the implants (Fig. 5A). Interestingly, compared with BSA controls, the presence of MHC II^{hi} or MHC II^{low} TAMs significantly increased the number of implant-directed vessels, demonstrating a proangiogenic activity for both TAM subsets. However, the vessel count for implants containing MHC II^{low} TAMs was on average 2-fold higher than with MHC II^{hi} TAMs. These data show that MHC II^{low} TAMs had a superior proangiogenic activity *in vivo*.

TAMs are poor antigen presenters, but can efficiently suppress T-cell proliferation

We wondered whether the TAM subsets were able to process internalized antigens and activate T cells. Both TAM subsets took up and processed DQ-Ovalbumin at 37°C. However, examining DQ-Ovalbumin processing at consecutive time points indicated that processing occurred more slowly in the MHC II^{low} fraction (Supplementary Fig. S9). To investigate whether TAMs could directly activate naive T cells, a MLR assay was used. Sorted MHC II^{hi} or MHC II^{low} TAMs were cultured with purified allogeneic C57BL/6 CD4$^+$ or CD8$^+$ T cells. Sorted splenic CD11c^{hi}MHC II^{hi} conventional dendritic cells (Supplementary Fig. S3D) were used as a reference T-cell–stimulating population (27). Compared with conventional dendritic cells, MHC II^{hi} or MHC II^{low} TAMs induced poor proliferation of allogeneic CD4$^+$ or CD8$^+$ T cells (Fig. 5B), suggesting a limited antigen-presenting capacity or, alternatively, a T-cell suppressive capacity that overrules antigen presentation.

To investigate the latter possibility, T cells were polyclonally activated in the presence of TAMs or conventional dendritic cells. Interestingly, as opposed to conventional dendritic cells, both MHC II^{hi} and MHC II^{low} TAMs equally suppressed anti–CD3-induced T-cell proliferation in a dose-dependent manner (Fig. 5C). In an attempt to identify the suppressive molecules responsible for TAM-mediated suppression, inhibitors of iNOS (L-NMMA) and arginase (Nor-Noha) were added to the cocultures (Fig. 5D). Blocking iNOS significantly reduced T-cell suppression by MHC II^{hi} TAMs, demonstrating a role for nitric oxide in its suppressive mechanism. In contrast, iNOS inhibition only had a minor effect on the suppressive potential of MHC II^{low} TAMs, showing that both subsets use different T-cell suppressive mechanisms.

Discussion

In this article, we show that the tumor-infiltrating myeloid compartment can be highly heterogeneous, with the coexistence of distinct subsets of granulocytes and mononuclear phagocytes. Furthermore, we identified the nature and dynamics of the monocyte precursor that was seeding tumors and giving rise to distinct TAM subsets. Interestingly, these subsets differed at the molecular and functional levels and were present in different intratumoral microenvironments (for an overview, see Supplementary Fig. S10).

Within the tumor-infiltrating monocyte pool, Ly6C^{hi}CX$_3$CR1^{int} monocytes were the most prominent subset, whereas Ly6C^{low}CX$_3$CR1^{hi} monocytes constituted only a small minority. In addition, bead labeling and BrdUrd incorporation experiments showed that Ly6C^{hi} monocytes were the precursors of all the distinct TAM subsets in TS/A tumors. Ly6C^{hi} monocytes rely on the chemokine receptor CCR2 for their migration from the bone marrow into the circulation (28). Recent studies showing that tumors grown in CCR2$^{-/-}$ mice have significantly reduced numbers of TAMs (29, 30) are therefore in line with our observation that Ly6C^{hi} monocytes comprise the main tumor-infiltrating monocyte subset. Furthermore, TAMs (and in particular MHC II^{low} TAMs) had a high gene expression of the CCR2 ligands *CCL2, CCL7*, and *CCL8*, suggesting an active role in the recruitment of Ly6C^{hi} monocytes. Most studies focusing on infection or immunization settings show that, at the site of insult, Ly6C^{hi} monocytes give rise to inflammatory dendritic cells (31–34). These inflammatory dendritic cells remain Ly6C^{hi}, express intermediate levels of CD11c, and can be efficient antigen presenters. In addition, a recent study has shown that shortly after *Listeria monocytogenes* infection, Ly6C^{hi} and Ly6C^{low} monocytes enter a dendritic cell or a macrophage differentiation program, respectively (35). However, our results show that at the tumor site, Ly6C^{hi} monocytes exclusively gave rise to distinct subsets of inflammatory macrophages, further highlighting monocyte plasticity and the impact of the tumor microenvironment thereon.

Strikingly, MHC II^{hi} and MHC II^{low} TS/A TAMs tended to be more M1- or M2-like, respectively. At the protein level, this included the differential expression of the M1 markers MHC II, CD11c, and iNOS, and the typical M2 markers MMR, SR-A, IL-4Rα, and arginase-1. Further proof for a differential activation state was delivered by gene expression analysis: an upregulation of proinflammatory genes in MHC II^{hi} TAMs, whereas M2-associated genes preferentially adhered to the MHC II^{low} subset. Interestingly, Hagemann and colleagues described that macrophages cocultured with ovarian cancer cells obtain an M2-like phenotype reminiscent of the MHC II^{low} TAMs in our present study, including upregulation of MMR, SR-A, and high expression levels of TNFα (23). In follow-up studies, it was shown that inhibiting IκB kinase (IKK) β activity in these macrophages results in a switch from M2 to M1, as evidenced by enhanced expression of MHC II, iNOS, and IL-12, and a reduction in arginase, TNFα, and IL-4Rα (24, 36). Hence, MHC II^{hi} TAMs more closely resemble the phenotype of the IKKβ-deficient macrophages, raising the possibility that the opposing activation states of MHC II^{hi} and MHC II^{low} TAMs might be driven by a differential NF-κB activity in these subsets.

Importantly, our findings in TS/A could be translated to 4T1 and 3LL tumors. The remarkable similarities between

Published OnlineFirst June 22, 2010; DOI: 10.1158/0008-5472.CAN-09-4672

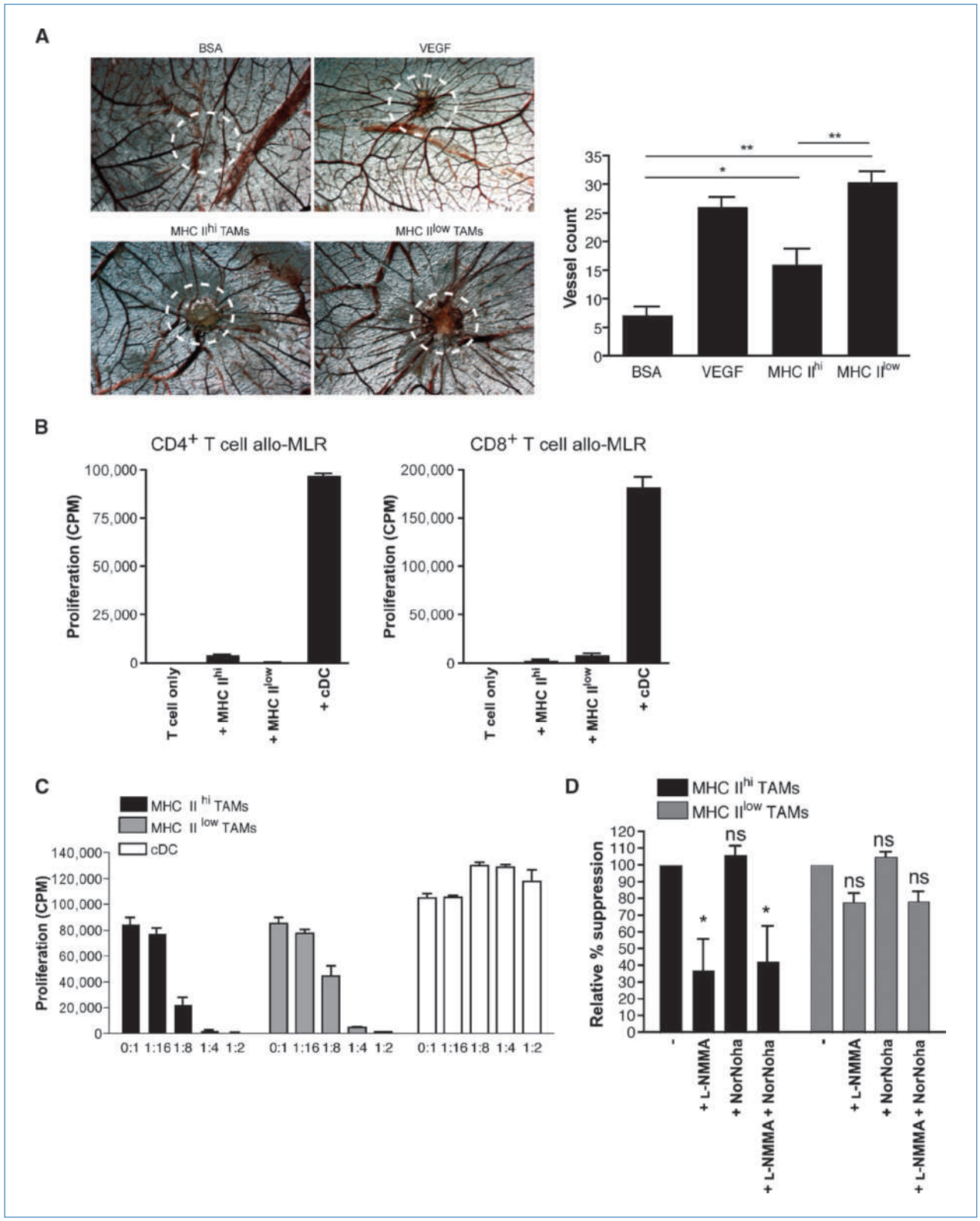

Figure 5. Differential functions of TAM subsets. A, sorted TAMs, BSA, and rhVEGF were grafted on CAMs. Numbers of implant-directed vessels were quantified (n = 2). B, allo-MLR assays with TAMs or BALB/c conventional dendritic cells (cDC). Average level of [^{3}H]thymidine incorporation (counts per minute, cpm) is shown (n = 3). C, suppression of syngeneic anti–CD3-induced T-cell proliferation by TAMs or conventional dendritic cells (n = 3). D, influence of indicated inhibitors on TAM-mediated suppression. ns, not significant.

Published OnlineFirst June 22, 2010; DOI: 10.1158/0008-5472.CAN-09-4672

TAM subsets from these unrelated tumors suggest that similar environmental cues might shape their respective phenotypes.

Interestingly, in TS/A tumors, MHC II^{low} TAMs were found to preferentially reside in hypoxic regions, as shown by pimonidazole stainings and their reduced access to blood-transported molecules. Hypoxia is known to influence gene and protein expression of macrophages: inducing expression of arginase, TNF, and proangiogenic factors while downregulating MHC II (37–39). Hypoxia-inducible factors (HIF) are the main transcription factors involved in regulating hypoxia-driven gene expression (26). Interestingly, a recent report showed that IKKβ is required for HIF-1α accumulation under hypoxic conditions, thereby uncovering a link between the hypoxic response and NF-κB (40). Hence, it is tempting to speculate that the involvement of IKKβ in shaping the M2 activation state of macrophages and its requirement for HIF-1α activity might be involved in the M2 skewing of hypoxic TAMs. Irrespective of the molecular mechanism, these are the first data linking the M2-like orientation of TAMs with a hypoxic environment.

Another striking difference between TS/A MHC II^{hi} and MHC II^{low} TAMs was at the level of chemokine and chemokine receptor expression. MHC II^{low} TAMs, possibly under the influence of hypoxia, had the highest gene expression of monocyte-recruiting chemokines, whereas chemokines that can recruit Th1, Th2, or natural killer cells, such as *Cx$_3$cl1, Ccl5, Cxcl9, Cxcl10, Cxcl11, Ccl17*, and *Ccl22* (41), were clearly upregulated in MHC II^{hi} TAMs. Hence, TAM subsets might contribute differently to shaping the inflammatory tumor infiltrate. In addition, the differential membrane expression of CX$_3$CR1 and CCR2 on the TAM subsets possibly reflects the use of different chemokine axes for their migration.

A recent study compared the gene expression profile of tumor-associated CD11b$^+$Tie2$^+$ cells (TEM) with that of CD11b$^+$Tie2$^-$ cells (42). Remarkably, many of the genes that are differentially expressed between TEMs and the residual CD11b$^+$ fraction were also key differential genes between MHC II^{low} and MHC II^{hi} TAMs. For example, similar to MHC II^{low} TAMs, TEMs have a higher mRNA expression level of *Lyve1, CD163, Stab1, Mrc1, Arg1*, and *Il4Ra*, but lower *Il1b, Nos2, Ptgs2, Ccl5, Cxcl10*, and *Cxcl11*. However, TEMs are only a minor fraction of CD11b$^+$ cells in tumors and are suggested to have a lineage relationship with Ly6C^{low}CX$_3$CR1^{hi} monocytes (42). In contrast, MHC II^{low} TAMs were the most abundant tumor-associated myeloid population and were originating from Ly6C^{hi} monocytes. In addition, antibody staining did not reveal any Tie-2 expression on MHC II^{low} TAMs and Tie2 mRNA levels were slightly lower in MHC II^{low} compared with MHC II^{hi} TAMs. Although we do not exclude that TEMs might be present in the MHC II^{low} fraction, our results suggest that MHC II^{low} TAMs and TEMs are distinct populations, but have intriguing similarities in their phenotypes. Because TEMs are potent proangiogenic cells (43), it is tempting to speculate that the similarities between TEMs and MHC II^{low} TAMs might reflect a comparable function. Indeed, one of the key responses to hypoxia is the induction of an angiogenic program (26).

An *in vivo* CAM assay showed that both TS/A TAM subsets stimulated angiogenesis. Interestingly, however, in line with their localization in hypoxic regions, MHC II^{low} TAMs showed a significantly higher proangiogenic activity, indicating that the balance of proangiogenic versus antiangiogenic mediators was highest for this subset. At present, the exact molecular basis for the increased angiogenic potential of MHC II^{low} TAMs is not clear, as several proangiogenic genes were expressed at a high level in both TAM populations. However, MHC II^{hi} TAMs had the highest expression of the antiangiogenic CXC chemokines (*Cxcl9-11*; ref. 44), potentially limiting the effects of proangiogenic factors.

The induction of myeloid-derived suppressor cells (MDSC) is shown to be an important immune-evading strategy used by tumors (45, 46). We and others have previously shown that splenic CD11b$^+$Gr-1$^+$ MDSCs consist of two major subsets: monocytic Ly6G$^-$ MO-MDSCs and granulocytic Ly6G$^+$ PMN-MDSCs (19, 47). Importantly, the phenotype of TS/A tumor-infiltrating Ly6C^{hi}(MHC II$^-$) monocytes closely resembled that of MO-MDSCs, whereas the tumor-infiltrating Ly6G$^+$ neutrophils were reminiscent of PMN-MDSCs (19). However, whether these tumor-infiltrating cells have immune-suppressive potential remains to be determined. In any case, within the TS/A tumor microenvironment, cells with a MO-MDSC–like phenotype differentiate into CD11b$^+$Gr-1$^-$/Ly6C$^-$ macrophages, suggesting a potential lineage relationship between MDSCs and TAMs. Importantly, T-cell–suppressive activity was a prominent feature of TAMs. Indeed, whereas MHC II^{hi} and MHC II^{low} TAMs were able to process antigens (albeit with different kinetics), they inefficiently activated naive T cells. In contrast, both subsets strongly suppressed polyclonal T-cell proliferation. Interestingly, in line with their M1-like activation, MHC II^{hi} TAMs relied to a higher extent on iNOS for suppression.

It has been predicted that TAMs in different tumor regions might have specialized functions (4). Our results provide the first evidence for this and describe markers for their discrimination in three independent tumor models. This offers the prospect of specifically targeting the M1-/M2-like or hypoxic/perivascular TAM subsets and investigating their impact on tumor biology. Eventually, this might lead to combinatorial strategies for optimally "re-educating" the TAM compartment and reverting its tumor-promoting activities.

Disclosure of Potential Conflicts of Interest

No potential conflicts of interest were disclosed.

Grant Support

Doctoral grants from FWO-Vlaanderen (K. Movahedi and J. Van den Bossche), a doctoral grant from IWT-Vlaanderen (D. Laoui), and grants from Stichting tegen Kanker.

The costs of publication of this article were defrayed in part by the payment of page charges. This article must therefore be hereby marked *advertisement* in accordance with 18 U.S.C. Section 1734 solely to indicate this fact.

Received 12/23/2009; revised 04/15/2010; accepted 04/30/2010; published OnlineFirst 06/22/2010.

Published OnlineFirst June 22, 2010; DOI: 10.1158/0008-5472.CAN-09-4672

References

1. Mantovani A, Allavena P, Sica A, Balkwill F. Cancer-related inflammation. Nature 2008;454:436–44.
2. Pollard JW. Tumour-educated macrophages promote tumour progression and metastasis. Nat Rev Cancer 2004;4:71–8.
3. Lin EY, Li JF, Gnatovskiy L, et al. Macrophages regulate the angiogenic switch in a mouse model of breast cancer. Cancer Res 2006; 66:11238–46.
4. Lewis CE, Pollard JW. Distinct role of macrophages in different tumor microenvironments. Cancer Res 2006;66:605–12.
5. Varol C, Yona S, Jung S. Origins and tissue-context-dependent fates of blood monocytes. Immunol Cell Biol 2009;87:30–8.
6. Auffray C, Sieweke MH, Geissmann F. Blood monocytes: development, heterogeneity, and relationship with dendritic cells. Annu Rev Immunol 2009;27:669–92.
7. Martinez FO, Helming L, Gordon S. Alternative activation of macrophages: an immunologic functional perspective. Annu Rev Immunol 2009;27:451–83.
8. Sica A, Schioppa T, Mantovani A, Allavena P. Tumour-associated macrophages are a distinct M2 polarised population promoting tumour progression: potential targets of anti-cancer therapy. Eur J Cancer 2006;42:717–27.
9. Lewis C, Murdoch C. Macrophage responses to hypoxia: implications for tumor progression and anti-cancer therapies. Am J Pathol 2005;167:627–35.
10. Nanni P, de Giovanni C, Lollini PL, Nicoletti G, Prodi G. TS/A: a new metastasizing cell line from a BALB/c spontaneous mammary adenocarcinoma. Clin Exp Metastasis 1983;1:373–80.
11. Pulaski BA, Ostrand-Rosenberg S. Mouse 4T1 breast tumor model. Curr Protoc Immunol 2001. Chapter 20:Unit 20.2.
12. Remels LM, De Baetselier PC. Characterization of 3LL-tumor variants generated by *in vitro* macrophage-mediated selection. Int J Cancer 1987;39:343–52.
13. Liu Y, Van Ginderachter JA, Brys L, De Baetselier P, Raes G, Geldhof AB. Nitric oxide-independent CTL suppression during tumor progression: association with arginase-producing (M2) myeloid cells. J Immunol 2003;170:5064–74.
14. Tacke F, Ginhoux F, Jakubzick C, van Rooijen N, Merad M, Randolph GJ. Immature monocytes acquire antigens from other cells in the bone marrow and present them to T cells after maturing in the periphery. J Exp Med 2006;203:583–97.
15. Tacke F, Alvarez D, Kaplan TJ, et al. Monocyte subsets differentially employ CCR2, CCR5, and CX3CR1 to accumulate within atherosclerotic plaques. J Clin Invest 2007;117:185–94.
16. Van Rooijen N, Sanders A. Liposome mediated depletion of macrophages: mechanism of action, preparation of liposomes and applications. J Immunol Methods 1994;174:83–93.
17. Van Ginderachter JA, Meerschaut S, Liu Y, et al. Peroxisome proliferator-activated receptor γ (PPARγ) ligands reverse CTL suppression by alternatively activated (M2) macrophages in cancer. Blood 2006;108:525–35.
18. Movahedi B, Gysemans C, Jacobs-Tulleneers-Thevissen D, Mathieu C, Pipeleers D. Pancreatic duct cells in human islet cell preparations are a source of angiogenic cytokines interleukin-8 and vascular endothelial growth factor. Diabetes 2008;57:2128–36.
19. Movahedi K, Guilliams M, Van den Bossche J, et al. Identification of discrete tumor-induced myeloid-derived suppressor cell subpopulations with distinct T cell-suppressive activity. Blood 2008;111: 4233–44.
20. Scholzen T, Gerdes J. The Ki-67 protein: from the known and the unknown. J Cell Physiol 2000;182:311–22.
21. Ojalvo LS, King W, Cox D, Pollard JW. High-density gene expression analysis of tumor-associated macrophages from mouse mammary tumors. Am J Pathol 2009;174:1048–64.
22. Biswas SK, Gangi L, Paul S, et al. A distinct and unique transcriptional program expressed by tumor-associated macrophages (defective NF-κB and enhanced IRF-3/STAT1 activation). Blood 2006;107: 2112–22.
23. Hagemann T, Wilson J, Burke F, et al. Ovarian cancer cells polarize macrophages toward a tumor-associated phenotype. J Immunol 2006;176:5023–32.
24. Hagemann T, Lawrence T, McNeish I, et al. "Re-educating" tumor-associated macrophages by targeting NF-κB. J Exp Med 2008; 205:1261–8.
25. Cho CH, Koh YJ, Han J, et al. Angiogenic role of LYVE-1-positive macrophages in adipose tissue. Circ Res 2007;100:e47–57.
26. Pugh CW, Ratcliffe PJ. Regulation of angiogenesis by hypoxia: role of the HIF system. Nat Med 2003;9:677–84.
27. Reis e Sousa C. Dendritic cells in a mature age. Nat Rev Immunol 2006;6:476–83.
28. Serbina NV, Pamer EG. Monocyte emigration from bone marrow during bacterial infection requires signals mediated by chemokine receptor CCR2. Nat Immunol 2006;7:311–7.
29. Sawanobori Y, Ueha S, Kurachi M, et al. Chemokine-mediated rapid turnover of myeloid-derived suppressor cells in tumor-bearing mice. Blood 2008;111:5457–66.
30. Pahler JC, Tazzyman S, Erez N, et al. Plasticity in tumor-promoting inflammation: impairment of macrophage recruitment evokes a compensatory neutrophil response. Neoplasia 2008;10:329–40.
31. Guilliams M, Movahedi K, Bosschaerts T, et al. IL-10 dampens TNF/inducible nitric oxide synthase-producing dendritic cell-mediated pathogenicity during parasitic infection. J Immunol 2009;182: 1107–18.
32. Auffray C, Fogg DK, Narni-Mancinelli E, et al. CX3CR1$^+$ CD115$^+$ CD135$^+$ common macrophage/DC precursors and the role of CX3CR1 in their response to inflammation. J Exp Med 2009;206: 595–606.
33. Kool M, Soullie T, van Nimwegen M, et al. Alum adjuvant boosts adaptive immunity by inducing uric acid and activating inflammatory dendritic cells. J Exp Med 2008;205:869–82.
34. Nakano H, Lin KL, Yanagita M, et al. Blood-derived inflammatory dendritic cells in lymph nodes stimulate acute T helper type 1 immune responses. Nat Immunol 2009;10:394–402.
35. Auffray C, Fogg D, Garfa M, et al. Monitoring of blood vessels and tissues by a population of monocytes with patrolling behavior. Science 2007;317:666–70.
36. Fong CH, Bebien M, Didierlaurent A, et al. An antiinflammatory role for IKKβ through the inhibition of "classical" macrophage activation. J Exp Med 2008;205:1269–76.
37. Murdoch C, Muthana M, Lewis CE. Hypoxia regulates macrophage functions in inflammation. J Immunol 2005;175:6257–63.
38. Mancino A, Schioppa T, Larghi P, et al. Divergent effects of hypoxia on dendritic cell functions. Blood 2008;112:3723–34.
39. Danet GH, Pan Y, Luongo JL, Bonnet DA, Simon MC. Expansion of human SCID-repopulating cells under hypoxic conditions. J Clin Invest 2003;112:126–35.
40. Rius J, Guma M, Schachtrup C, et al. NF-κB links innate immunity to the hypoxic response through transcriptional regulation of HIF-1α. Nature 2008;453:807–11.
41. Mantovani A, Sica A, Sozzani S, Allavena P, Vecchi A, Locati M. The chemokine system in diverse forms of macrophage activation and polarization. Trends Immunol 2004;25:677–86.
42. Pucci F, Venneri MA, Biziato D, et al. A distinguishing gene signature shared by tumor-infiltrating Tie2-expressing monocytes, blood "resident" monocytes, and embryonic macrophages suggests common functions and developmental relationships. Blood 2009;114:901–14.
43. De Palma M, Murdoch C, Venneri MA, Naldini L, Lewis CE. Tie2-expressing monocytes: regulation of tumor angiogenesis and therapeutic implications. Trends Immunol 2007;28:519–24.
44. Belperio JA, Keane MP, Arenberg DA, et al. CXC chemokines in angiogenesis. J Leukoc Biol 2000;68:1–8.
45. Gabrilovich DI, Nagaraj S. Myeloid-derived suppressor cells as regulators of the immune system. Nat Rev Immunol 2009;9:162–74.
46. Ostrand-Rosenberg S, Sinha P. Myeloid-derived suppressor cells: linking inflammation and cancer. J Immunol 2009;182:4499–506.
47. Youn JI, Nagaraj S, Collazo M, Gabrilovich DI. Subsets of myeloid-derived suppressor cells in tumor-bearing mice. J Immunol 2008; 181:5791–802.

Published OnlineFirst June 22, 2010; DOI: 10.1158/0008-5472.CAN-09-4672

AACR American Association for Cancer Research

Cancer Research

The Journal of Cancer Research (1916–1930) | The American Journal of Cancer (1931–1940)

Different Tumor Microenvironments Contain Functionally Distinct Subsets of Macrophages Derived from Ly6C(high) Monocytes

Kiavash Movahedi, Damya Laoui, Conny Gysemans, et al.

Cancer Res 2010;70:5728-5739. Published OnlineFirst June 22, 2010.